Neutrino and Nuclear Properties from Coherent Elastic Neutrino-Nucleus Scattering

Carlo Giunti
INFN, Torino, Italy

Seminar at IPN

26 September 2018, Orsay

Coherent Elastic Neutrino-Nucleus Scattering

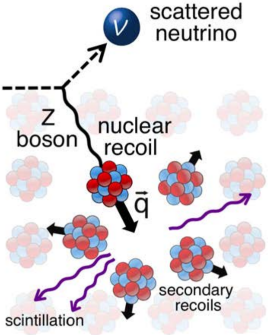

- Predicted in 1974 for $|\vec{q}|R \lesssim 1$
  [Freedman, PRD 9 (1974) 1389]

- $$\frac{d\sigma}{dT}(E_\nu, T) \simeq \frac{G_F^2 M}{4\pi}\left(1 - \frac{MT}{2E_\nu^2}\right) N^2 F_N^2(|\vec{q}|^2)$$
  [Drukier, Stodolski, PRD (1984) 2295]

- Observed in 2017 in the COHERENT experiment at the Oak Ridge Spallation Neutron Source with CsI ($N_{\mathrm{Cs}} = 78$, $N_{\mathrm{I}} = 74$)
  [Science 357 (2017) 1123, arXiv:1708.01294]

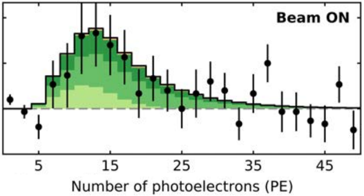

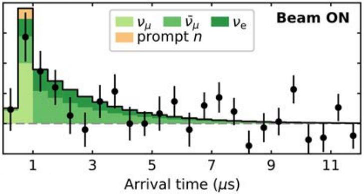

- Several oncoming new experiments: CONUS, CONNIE, NU-CLEUS, MINER, Ricochet, TEXONO, νGEN

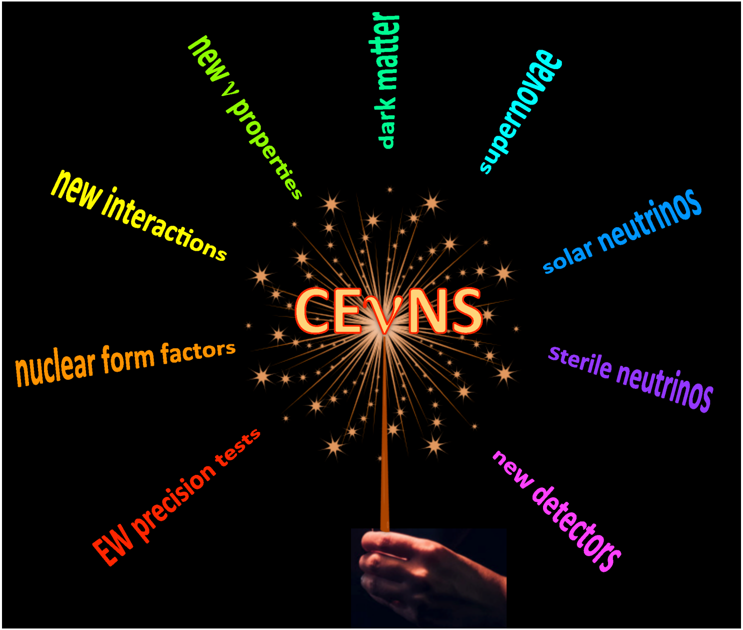

[E. Lisi, Neutrino 2018]

- Taking into account interactions with both neutrons and protons

$$\frac{d\sigma}{dT}(E_\nu, T) = \frac{G_F^2 M}{\pi}\left(1 - \frac{MT}{2E_\nu^2}\right)\left[g_V^n N F_N(|\vec{q}|^2) + g_V^p Z F_Z(|\vec{q}|^2)\right]^2$$

$$g_V^n = -\frac{1}{2} \qquad g_V^p = \frac{1}{2} - 2\sin^2\vartheta_W = 0.0227 \pm 0.0002$$

The neutron contribution is dominant! $\Longrightarrow$ $\frac{d\sigma}{dT} \sim N^2 F_N^2(|\vec{q}|^2)$

- The form factors $F_N(|\vec{q}|^2)$ and $F_Z(|\vec{q}|^2)$ describe the loss of coherence for $|\vec{q}|R \gtrsim 1$. [see: Bednyakov, Naumov, arXiv:1806.08768]

- Coherence requires very small values of the nuclear kinetic recoil energy $T \simeq |\vec{q}|^2/2M$:

$$|\vec{q}|R \lesssim 1 \quad \Longleftrightarrow \quad T \lesssim \frac{1}{2MR^2}$$

$$M \approx 100\,\text{GeV}, \quad R \approx 5\,\text{fm} \quad \Longrightarrow \quad T \lesssim 10\,\text{keV}$$

The COHERENT Experiment

Oak Ridge Spallation Neutron Source

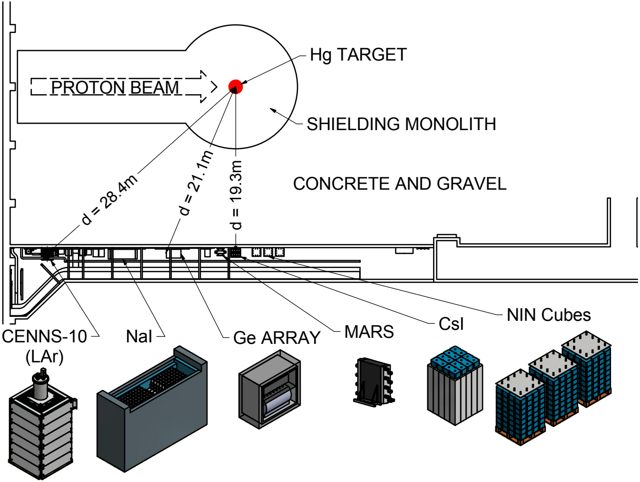

14.6 kg CsI
scintillating crystal

[COHERENT, arXiv:1803.09183]

COHERENT Neutrino Spectrum

Neutrinos at the Oak Ridge Spallation Neutron Source are produced by a pulsed proton beam striking a mercury target.

- Prompt monochromatic ν_μ from stopped pion decays:

$$\pi^+ \to \mu^+ + \nu_\mu$$

$$\frac{dN_{\nu_\mu}}{dE_\nu} = \eta\,\delta\left(E_\nu - \frac{m_\pi^2 - m_\mu^2}{2m_\pi}\right)$$

- Delayed $\bar{\nu}_\mu$ and ν_e from the subsequent muon decays:

$$\mu^+ \to e^+ + \bar{\nu}_\mu + \nu_e$$

$$\frac{dN_{\nu_{\bar{\mu}}}}{dE_\nu} = \eta\,\frac{64E_\nu^2}{m_\mu^3}\left(\frac{3}{4} - \frac{E_\nu}{m_\mu}\right)$$

$$\frac{dN_{\nu_e}}{dE_\nu} = \eta\,\frac{192E_\nu^2}{m_\mu^3}\left(\frac{1}{2} - \frac{E_\nu}{m_\mu}\right)$$

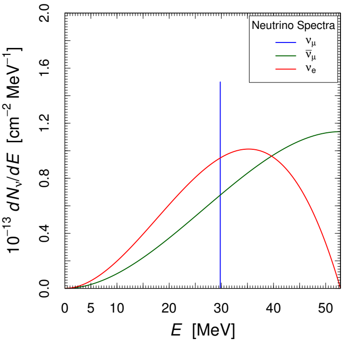

- From kinematics $T < 2E_\nu^2/M$
- $E_\nu \leq \frac{m_\mu}{2} \simeq 52.8\,\text{MeV}$

$$\Downarrow$$

$$T \lesssim 50\,\text{keV}$$

Cross Section

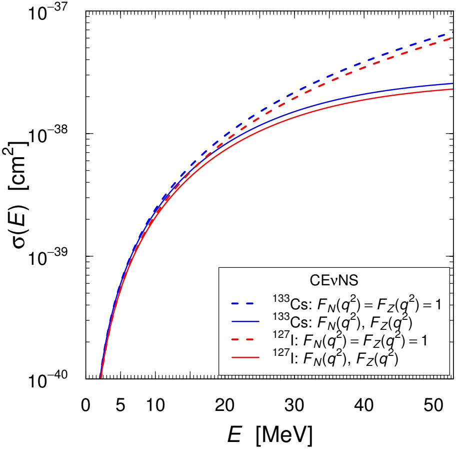

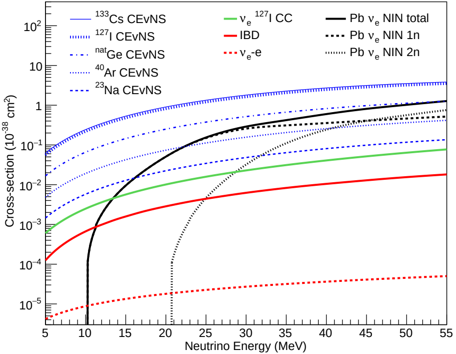

[COHERENT, arXiv:1803.09183]

- In the COHERENT experiment neutrino-nucleus scattering is not completely coherent:

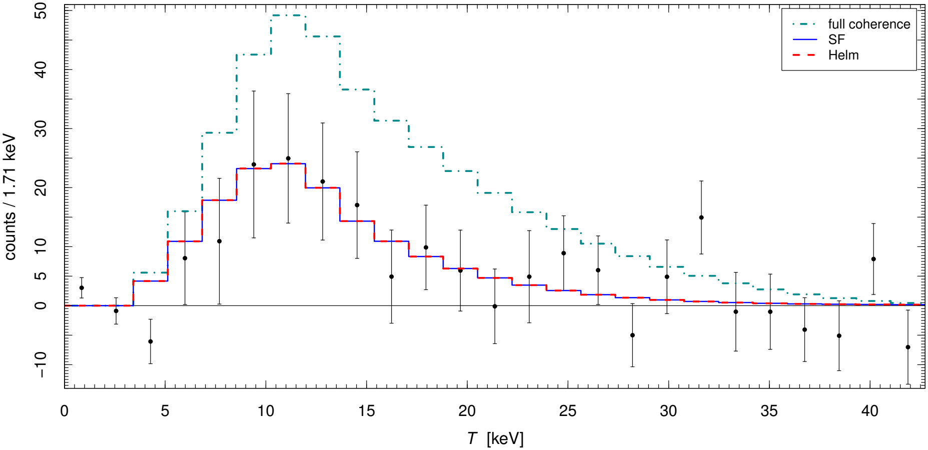

[Cadeddu, CG, Y.F. Li, Y.Y. Zhang, PRL 120 (2018) 072501, arXiv:1710.02730]

- Partial coherency gives information on the nuclear neutron form factor $F_N(|\vec{q}|^2)$, which is the Fourier transform of the neutron distribution in the nucleus.

Helm form factor: $F_N^{\text{Helm}}(|\vec{q}|^2) = 3\,\frac{j_1(|\vec{q}|R_0)}{|\vec{q}|R_0}\,e^{-|\vec{q}|^2 s^2/2}$

Spherical Bessel function of order one: $j_1(x) = \sin(x)/x^2 - \cos(x)/x$

Obtained from the convolution of a sphere with constant density with radius R_0 and a gaussian density with standard deviation s

Rms radius: $R^2 = \langle r^2 \rangle = \frac{3}{5}\,R_0^2 + 3s^2$

Surface thickness: $s \simeq 0.9\,\text{fm}$

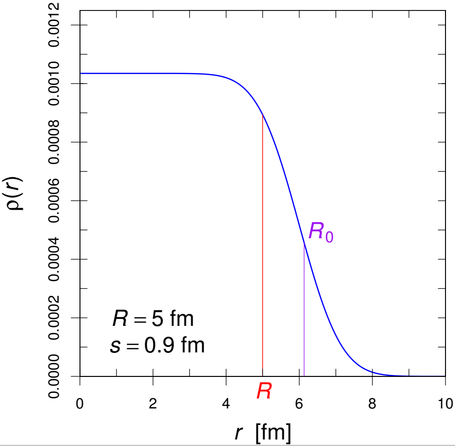

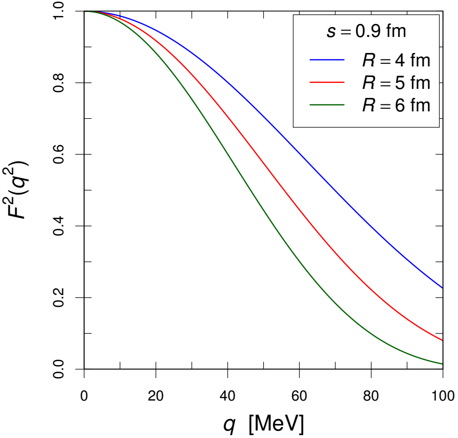

Helm form factor: $F_N^{\text{Helm}}(|\vec{q}|^2) = 3\,\frac{j_1(|\vec{q}|R_0)}{|\vec{q}|R_0}\,e^{-|\vec{q}|^2 s^2/2}$

Spherical Bessel function of order one: $j_1(x) = \sin(x)/x^2 - \cos(x)/x$

Obtained from the convolution of a sphere with constant density with radius R_0 and a gaussian density with standard deviation s

Rms radius: $R^2 = \langle r^2 \rangle = \frac{3}{5}\,R_0^2 + 3s^2$

Surface thickness: $s \simeq 0.9\,\text{fm}$

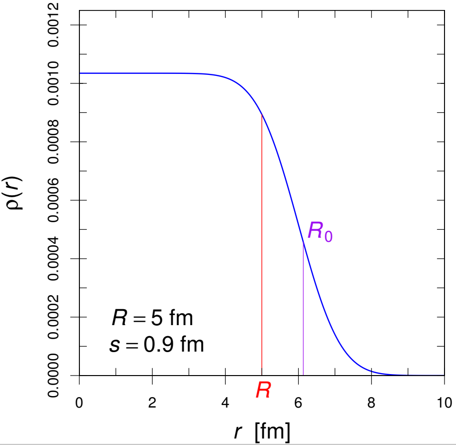

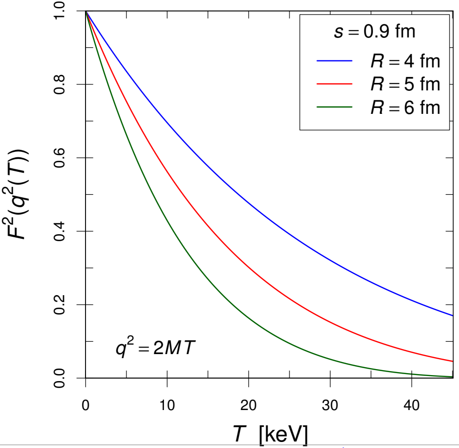

The Nuclear Proton and Neutron Distributions

- The nuclear proton distribution (charge density) is probed with electromagnetic interactions.
- Most sensitive are electron-nucleus elastic scattering and muonic atom spectroscopy.
- Hadron scattering experiments give information on the nuclear neutron distribution, but their interpretation depends on the model used to describe non-perturbative strong interactions.
- More reliable are neutral current weak interaction measurements.
  But they are more difficult.
- Before 2017 there was only one measurement of R_n with neutral-current weak interactions through parity-violating electron scattering:

$$R_n(^{208}\mathrm{Pb}) = 5.78^{+0.16}_{-0.18}\,\mathrm{fm}$$

[PREX, PRL 108 (2012) 112502]

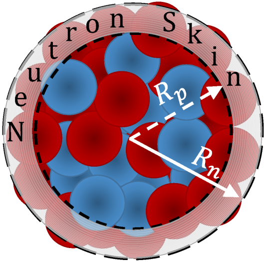

- The rms radii of the proton distributions of ^{133}Cs and ^{127}I have been determined with muonic atom spectroscopy: [Fricke et al, ADNDT 60 (1995) 177]

$$R_p^{(\mu)}(^{133}\mathrm{Cs}) = 4.804\,\mathrm{fm} \qquad R_p^{(\mu)}(^{127}\mathrm{I}) = 4.749\,\mathrm{fm}$$

- Fit of the COHERENT data to get $R_n(^{133}\mathrm{Cs}) \simeq R_n(^{127}\mathrm{I})$:

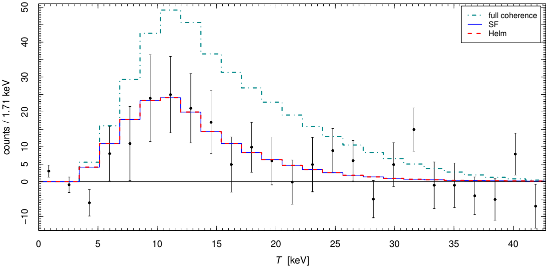

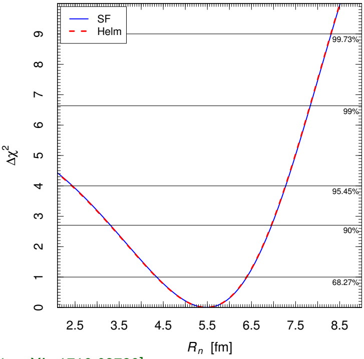

[Cadeddu, CG, Li, Zhang, PRL 120 (2018) 072501, arXiv:1710.02730]

$$\boxed{R_n(^{133}\mathrm{Cs}) \simeq R_n(^{127}\mathrm{I}) = 5.5^{+0.9}_{-1.1}\ \mathrm{fm}}$$

[Cadeddu, CG, Li, Zhang, PRL 120 (2018) 072501, arXiv:1710.02730]

- This is the first determination of R_n with neutrino-nucleus scattering.
- The uncertainty is large, but it can be improved in future experiments.
- Predictions of nonrelativistic Skyrme-Hartree-Fock (SHF) and relativistic mean field (RMF) nuclear models:

	^{133}Cs		^{127}I	
	R_p	R_n	R_p	R_n
SHF SkM*	4.76	4.90	4.71	4.84
SHF SkP	4.79	4.91	4.72	4.84
SHF SkI4	4.73	4.88	4.67	4.81
SHF Sly4	4.78	4.90	4.71	4.84
SHF UNEDF1	4.76	4.90	4.68	4.83
RMF NL-SH	4.74	4.93	4.68	4.86
RMF NL3	4.75	4.95	4.69	4.89
RMF NL-Z2	4.79	5.01	4.73	4.94
Exp. (μ-atom spect.)	4.804		4.749	

Electromagnetic Interactions

- Effective Hamiltonian: $\mathcal{H}_{\text{em}}^{(\nu)}(x) = j_\mu^{(\nu)}(x) A^\mu(x) = \sum_{k,j=1} \overline{\nu_k}(x) \Lambda_\mu^{kj} \nu_j(x) A^\mu(x)$

- Effective electromagnetic vertex:

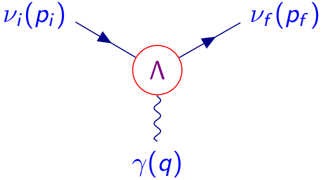

$$\langle \nu_f(p_f) | j_\mu^{(\nu)}(0) | \nu_i(p_i) \rangle = \overline{u_f}(p_f) \Lambda_\mu^{fi}(q) u_i(p_i)$$

$$q = p_i - p_f$$

- Vertex function:

$$\Lambda_\mu(q) = \left(\gamma_\mu - q_\mu \not{q}/q^2\right) \left[F_Q(q^2) + F_A(q^2) q^2 \gamma_5\right] - i \sigma_{\mu\nu} q^\nu \left[F_M(q^2) + i F_E(q^2) \gamma_5\right]$$

Lorentz-invariant form factors: charge, anapole, magnetic, electric

$q^2 = 0 \implies$ $\mathbb{q}$, a, μ, ε

- Hermitian form factor matrices $\implies$ $\mathbb{q} = \mathbb{q}^\dagger$ $\quad a = a^\dagger$ $\quad \mu = \mu^\dagger$ $\quad \varepsilon = \varepsilon^\dagger$

Electromagnetic Interactions

- Effective Hamiltonian: $\mathcal{H}_{\text{em}}^{(\nu)}(x) = j_{\mu}^{(\nu)}(x) A^{\mu}(x) = \sum_{k,j=1} \overline{\nu_k}(x) \Lambda_{\mu}^{kj} \nu_j(x) A^{\mu}(x)$

- Effective electromagnetic vertex:

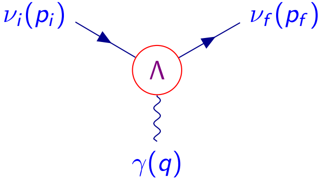

$$\langle \nu_f(p_f) | j_{\mu}^{(\nu)}(0) | \nu_i(p_i) \rangle = \overline{u_f}(p_f) \Lambda_{\mu}^{fi}(q) u_i(p_i)$$

$$q = p_i - p_f$$

- Vertex function:

$$\Lambda_{\mu}(q) = \left(\gamma_{\mu} - q_{\mu} \not{q}/q^2\right) \left[F_Q(q^2) + F_A(q^2) q^2 \gamma_5\right] - i\sigma_{\mu\nu} q^{\nu} \left[F_M(q^2) + i F_E(q^2) \gamma_5\right]$$

Lorentz-invariant form factors: charge, anapole, magnetic, electric

$q^2 = 0 \implies$ $\mathfrak{q}$, a, μ, ε

- Majorana neutrinos $\implies$ $\mathfrak{q} = -\mathfrak{q}^T \quad a = a^T \quad \mu = -\mu^T \quad \varepsilon = -\varepsilon^T$

  no diagonal charges and electric and magnetic moments

Electromagnetic Interactions

- Effective Hamiltonian: $\mathcal{H}_{\text{em}}^{(\nu)}(x) = j_\mu^{(\nu)}(x) A^\mu(x) = \sum_{k,j=1} \overline{\nu_k}(x) \Lambda_\mu^{kj} \nu_j(x) A^\mu(x)$

- Effective electromagnetic vertex:

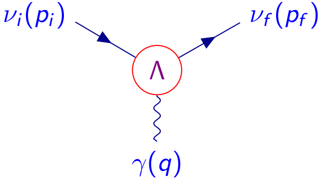

$$\langle \nu_f(p_f) | j_\mu^{(\nu)}(0) | \nu_i(p_i) \rangle = \overline{u_f}(p_f) \Lambda_\mu^{fi}(q) u_i(p_i)$$

$$q = p_i - p_f$$

- Vertex function:

$$\Lambda_\mu(q) = \left(\gamma_\mu - q_\mu \not{q}/q^2\right) \left[F_Q(q^2) + F_A(q^2) q^2 \gamma_5\right] - i\sigma_{\mu\nu} q^\nu \left[F_M(q^2) + i F_E(q^2) \gamma_5\right]$$

Lorentz-invariant form factors: charge, anapole, magnetic, electric

$q^2 = 0 \implies$ $\mathfrak{q}$, a, μ, ε

- For ultrarelativistic neutrinos $\gamma_5 \to -1 \Rightarrow$ The phenomenology of the charge and anapole moments are similar and the phenomenology of the magnetic and electric moments are similar.

Electromagnetic Interactions

- Effective Hamiltonian: $\mathcal{H}_{\text{em}}^{(\nu)}(x) = j_{\mu}^{(\nu)}(x) A^{\mu}(x) = \sum_{k,j=1} \overline{\nu_k}(x) \Lambda_{\mu}^{kj} \nu_j(x) A^{\mu}(x)$

- Effective electromagnetic vertex:

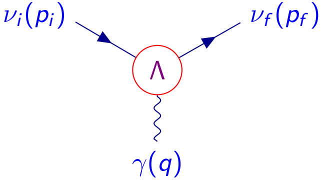

$$\langle \nu_f(p_f) | j_{\mu}^{(\nu)}(0) | \nu_i(p_i) \rangle = \overline{u_f}(p_f) \Lambda_{\mu}^{fi}(q) u_i(p_i)$$

$$q = p_i - p_f$$

- Vertex function:

$$\Lambda_{\mu}(q) = \left(\gamma_{\mu} - q_{\mu} \not{q}/q^2\right) \left[F_Q(q^2) + F_A(q^2) q^2 \gamma_5\right] - i \sigma_{\mu\nu} q^{\nu} \left[F_M(q^2) + i F_E(q^2) \gamma_5\right]$$

Lorentz-invariant form factors: charge, anapole, magnetic, electric

$q^2 = 0 \implies$ $\mathfrak{q}$, a, μ, ε

- For ultrarelativistic neutrinos the charge and anapole terms conserve helicity, whereas the magnetic and electric terms invert helicity.

Neutrino Charge Radius

- In the Standard Model neutrinos are neutral and there are no electromagnetic interactions at the tree-level.

- Radiative corrections generate an effective electromagnetic interaction vertex

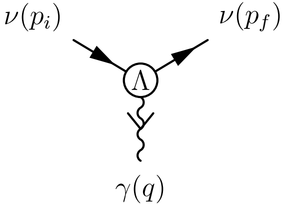

$$\Lambda_\mu(q) = \left(\gamma_\mu - q_\mu \not{q}/q^2\right) F(q^2)$$

- $F(q^2) = \cancel{F(0)} + q^2 \left. \frac{dF(q^2)}{dq^2} \right|_{q^2=0} + \ldots = q^2 \frac{\langle r^2 \rangle}{6} + \ldots$

- In the Standard Model: [Bernabeu et al, PRD 62 (2000) 113012, NPB 680 (2004) 450]

$$\langle r^2_{\nu_\ell} \rangle_{\mathrm{SM}} = -\frac{G_{\mathrm{F}}}{2\sqrt{2}\pi^2} \left[3 - 2 \log\left(\frac{m_\ell^2}{m_W^2} \right) \right]$$

Neutrino Charge Radius

- In the Standard Model neutrinos are neutral and there are no electromagnetic interactions at the tree-level.

- Radiative corrections generate an effective electromagnetic interaction vertex

$$\Lambda_\mu(q) = \left(\gamma_\mu - q_\mu \not{q}/q^2\right) F(q^2)$$

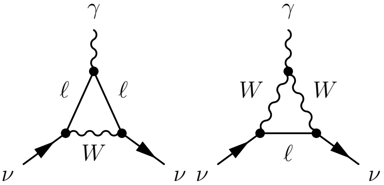

- $F(q^2) = \cancel{F(0)} + q^2 \left. \frac{dF(q^2)}{dq^2} \right|_{q^2=0} + \ldots = q^2 \frac{\langle r^2 \rangle}{6} + \ldots$

- In the Standard Model: [Bernabeu et al, PRD 62 (2000) 113012, NPB 680 (2004) 450]

$$\langle r^2_{\nu_\ell} \rangle_{\text{SM}} = -\frac{G_{\text{F}}}{2\sqrt{2}\pi^2}\left[3 - 2\log\left(\frac{m_\ell^2}{m_W^2}\right)\right]$$

Neutrino Charge Radius

- In the Standard Model neutrinos are neutral and there are no electromagnetic interactions at the tree-level.

- Radiative corrections generate an effective electromagnetic interaction vertex

$$\Lambda_\mu(q) = \left(\gamma_\mu - q_\mu \not{q}/q^2\right) F(q^2)$$

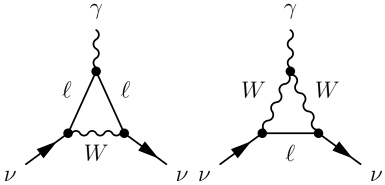

- $F(q^2) = \cancel{F(0)} + q^2 \left. \frac{dF(q^2)}{dq^2} \right|_{q^2=0} + \ldots = q^2 \frac{\langle r^2 \rangle}{6} + \ldots$

- In the Standard Model: [Bernabeu et al, PRD 62 (2000) 113012, NPB 680 (2004) 450]

$$\langle r^2_{\nu_e} \rangle_{\text{SM}} = -8.2 \times 10^{-33}\,\text{cm}^2 \quad \langle r^2_{\nu_\mu} \rangle_{\text{SM}} = -4.8 \times 10^{-33}\,\text{cm}^2 \quad \langle r^2_{\nu_\tau} \rangle_{\text{SM}} = -3.0 \times 10^{-33}\,\text{cm}^2$$

Experimental Bounds

Method	Experiment	Limit [cm^2]	CL	Year
Reactor $\bar{\nu}_e\, e^-$	Krasnoyarsk	$\lvert\langle r_{\nu_e}^2 \rangle\rvert < 7.3 \times 10^{-32}$	90%	1992
	TEXONO	$-4.2 \times 10^{-32} < \langle r_{\nu_e}^2 \rangle < 6.6 \times 10^{-32}$	90%	2009
Accelerator $\nu_e\, e^-$	LAMPF	$-7.12 \times 10^{-32} < \langle r_{\nu_e}^2 \rangle < 10.88 \times 10^{-32}$	90%	1992
	LSND	$-5.94 \times 10^{-32} < \langle r_{\nu_e}^2 \rangle < 8.28 \times 10^{-32}$	90%	2001
Accelerator $\nu_\mu\, e^-$	BNL-E734	$-4.22 \times 10^{-32} < \langle r_{\nu_\mu}^2 \rangle < 0.48 \times 10^{-32}$	90%	1990
	CHARM-II	$\lvert\langle r_{\nu_\mu}^2 \rangle\rvert < 1.2 \times 10^{-32}$	90%	1994

[see the review CG, Studenikin, RMP 87 (2015) 531, arXiv:1403.6344]

- Neutrino charge radii contributions to CEνNS $\nu_\ell + \mathcal{N} \to \nu_\ell + \mathcal{N}$:

$$\frac{d\sigma_{\nu_\ell\text{-}\mathcal{N}}}{dT}(E_\nu, T) = \frac{G_F^2 M}{\pi}\left(1 - \frac{MT}{2E_\nu^2}\right)\left\{\left[g_V^n N F_N(|\vec{q}|^2) + \left(g_V^p - \frac{2}{3}\, m_W^2 \sin^2\vartheta_W \langle r_{\nu_{\ell\ell}}^2\rangle\right) Z F_Z(|\vec{q}|^2)\right]^2 + \frac{4}{9}\, m_W^4 \sin^4\vartheta_W Z^2 F_Z^2(|\vec{q}|^2) \sum_{\ell' \neq \ell} |\langle r_{\nu_{\ell'\ell}}^2\rangle|^2\right\}$$

- In the Standard Model there are only diagonal charge radii $\langle r_{\nu_\ell}^2\rangle \equiv \langle r_{\nu_{\ell\ell}}^2\rangle$ because lepton numbers are conserved.
- Since $g_V^p = \frac{1}{2} - 2\sin^2\vartheta_W$, diagonal charge radii generate the coherent (helicity conserving) shifts

$$\sin^2\vartheta_W \to \sin^2\vartheta_W \left(1 + \frac{1}{3} m_W^2 \langle r_{\nu_\ell}^2\rangle\right)$$

- In general, the neutrino charge radius matrix $\langle r_\nu^2\rangle$ can be non-diagonal and the transition charge radii generate the incoherent contribution

$$\frac{4}{9}\, m_W^4 \sin^4\vartheta_W Z^2 F_Z^2(|\vec{q}|^2) \sum_{\ell' \neq \ell} |\langle r_{\nu_{\ell'\ell}}^2\rangle|^2 \quad \Longleftrightarrow \quad \nu_\ell + \mathcal{N} \to \sum_{\ell' \neq \ell} \nu_{\ell' \neq \ell} + \mathcal{N}$$

[Kouzakov, Studenikin, PRD 95 (2017) 055013, arXiv:1703.00401]

Fit of the COHERENT Energy Spectrum

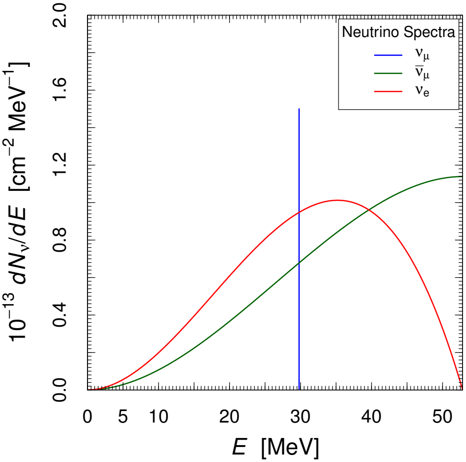

- The spectrum is especially sensitive to the difference of the properties of ν_μ and those of $\bar{\nu}_\mu$ and ν_e.
- Note that $\langle r^2_{\bar{\nu}_{\ell\ell'}} \rangle = -\langle r^2_{\nu_{\ell\ell'}} \rangle$.

Fit without transition charge radii

[Cadeddu, CG, Kouzakov, Y.F. Li, Studenikin, Y.Y. Zhang, in preparation]

Time-integrated COHERENT data

- Fixed neutron distribution radii (RMF NL-Z2):

$R_n(^{133}\mathrm{Cs}) = 5.01\,\mathrm{fm} \quad R_n(^{127}\mathrm{I}) = 4.94\,\mathrm{fm}$

$\chi^2_{\mathrm{min}} = 2.7 \quad \mathrm{NDF} = 10 \quad \mathrm{GoF} = 99\%$

Marginal 90% CL bounds $[10^{-32}\,\mathrm{cm}^2]$:

$-69 < \langle r^2_{\nu_e} \rangle < 19 \quad -15 < \langle r^2_{\nu_\mu} \rangle < 21$

- Free neutron distribution radii:

$\chi^2_{\mathrm{min}} = 2.5 \quad \mathrm{NDF} = 8 \quad \mathrm{GoF} = 96\%$

Marginal 90% CL bounds $[10^{-32}\,\mathrm{cm}^2]$:

$-69 < \langle r^2_{\nu_e} \rangle < 40 \quad -33 < \langle r^2_{\nu_\mu} \rangle < 38$

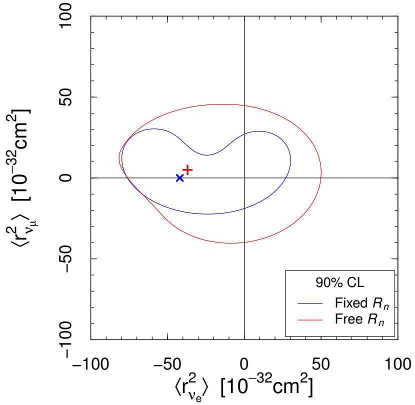

Fit with transition charge radii

[Cadeddu, CG, Kouzakov, Y.F. Li, Studenikin, Y.Y. Zhang, in preparation]

Time-integrated COHERENT data

- Fixed neutron distribution radii (RMF NL-Z2):

  $R_n(^{133}\mathrm{Cs}) = 5.01\,\mathrm{fm} \quad R_n(^{127}\mathrm{I}) = 4.94\,\mathrm{fm}$

  $\chi^2_{\mathrm{min}} = 2.6 \quad \mathrm{NDF} = 7 \quad \mathrm{GoF} = 92\%$

  Marginal 90% CL bounds $[10^{-32}\,\mathrm{cm}^2]$:

  $-69 < \langle r^2_{\nu_e} \rangle < 19 \quad -15 < \langle r^2_{\nu_\mu} \rangle < 22$

  $|\langle r^2_{\nu_{e\mu}} \rangle| < 25 \quad |\langle r^2_{\nu_{e\tau}} \rangle| < 44 \quad |\langle r^2_{\nu_{\mu\tau}} \rangle| < 31$

- Free neutron distribution radii:

  $\chi^2_{\mathrm{min}} = 2.5 \quad \mathrm{NDF} = 5 \quad \mathrm{GoF} = 77\%$

  Marginal 90% CL bounds $[10^{-32}\,\mathrm{cm}^2]$:

  $-69 < \langle r^2_{\nu_e} \rangle < 40 \quad -33 < \langle r^2_{\nu_\mu} \rangle < 38$

  $|\langle r^2_{\nu_{e\mu}} \rangle| < 29 \quad |\langle r^2_{\nu_{e\tau}} \rangle| < 49 \quad |\langle r^2_{\nu_{\mu\tau}} \rangle| < 36$

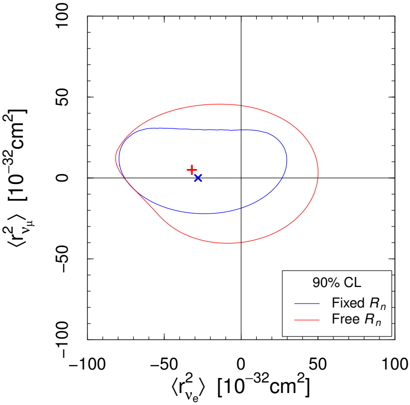

- Our results are different from those of
  Papoulias, Kosmas, PRD 97 (2018) 033003, arXiv:1711.09773
- Fitting only the total number of events:

Our Fit

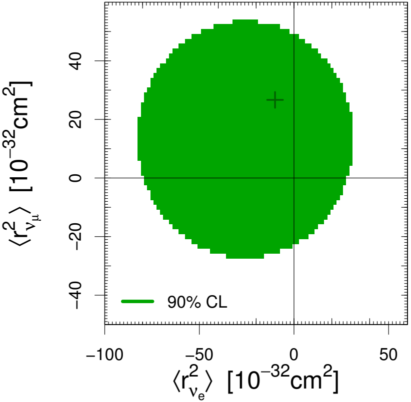

Papoulias & Kosmas

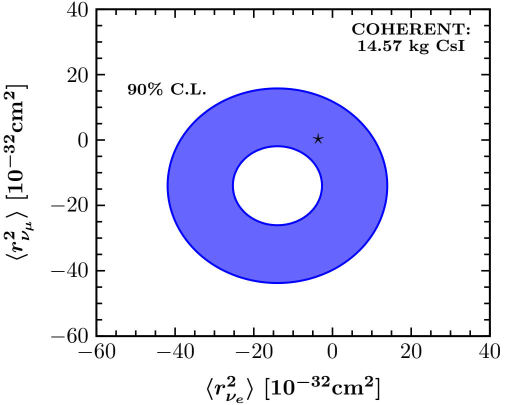

- A factor of 2 difference is due to different definitions of the charge radii.
- The shape difference may be due to the fact that they considered $\langle r^2_{\bar{\nu}_\ell} \rangle = \langle r^2_{\nu_\ell} \rangle \Leftrightarrow$ approximate $\langle r^2_{\nu_e} \rangle - \langle r^2_{\nu_\mu} \rangle$ symmetry.

COHERENT Time Distribution

- Prompt monochromatic ν_μ from stopped pion decays:

$$\pi^+ \to \mu^+ + \nu_\mu$$

- Delayed $\bar{\nu}_\mu$ and ν_e from the subsequent muon decays:

$$\mu^+ \to e^+ + \bar{\nu}_\mu + \nu_e$$

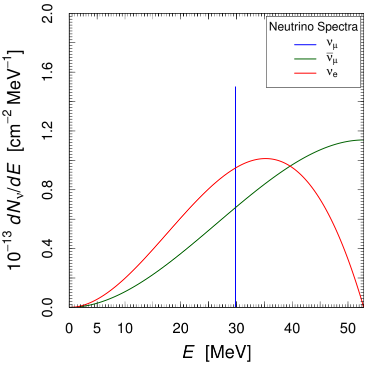

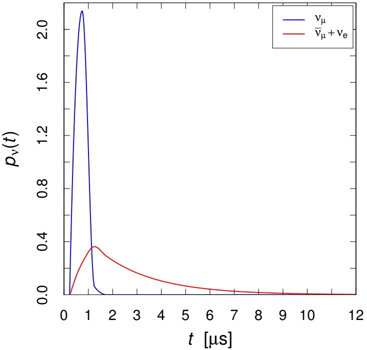

The time distribution of the data increases the information on the difference between the properties of ν_μ and those of $\bar{\nu}_\mu$ and ν_e.

Fit of Time-dependent COHERENT data

[Cadeddu, CG, Kouzakov, Y.F. Li, Studenikin, Y.Y. Zhang, in preparation]

- Fixed neutron distribution radii (RMF NL-Z2):

  $R_n(^{133}\mathrm{Cs}) = 5.01\,\mathrm{fm} \quad R_n(^{127}\mathrm{I}) = 4.94\,\mathrm{fm}$

  $\chi^2_{\mathrm{min}} = 154.2 \quad \mathrm{NDF} = 139 \quad \mathrm{GoF} = 18\%$

  Marginal 90% CL bounds $[10^{-32}\,\mathrm{cm}^2]$:

  $-63 < \langle r^2_{\nu_e} \rangle < 12 \quad -7 < \langle r^2_{\nu_\mu} \rangle < 9$

  $|\langle r^2_{\nu_{e\mu}} \rangle| < 22 \quad |\langle r^2_{\nu_{e\tau}} \rangle| < 37 \quad |\langle r^2_{\nu_{\mu\tau}} \rangle| < 26$

- Free neutron distribution radii:

  $\chi^2_{\mathrm{min}} = 153.7 \quad \mathrm{NDF} = 137 \quad \mathrm{GoF} = 16\%$

  Marginal 90% CL bounds $[10^{-32}\,\mathrm{cm}^2]$:

  $-61 < \langle r^2_{\nu_e} \rangle < 16 \quad -11 < \langle r^2_{\nu_\mu} \rangle < 22$

  $|\langle r^2_{\nu_{e\mu}} \rangle| < 26 \quad |\langle r^2_{\nu_{e\tau}} \rangle| < 40 \quad |\langle r^2_{\nu_{\mu\tau}} \rangle| < 30$

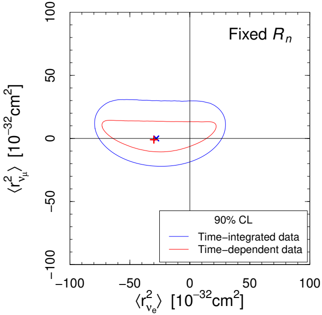

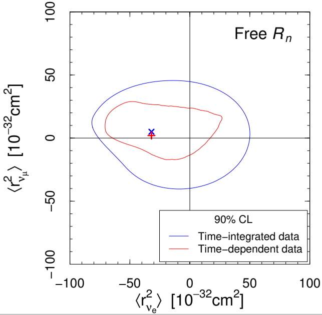

- The time-dependent spectral data of the COHERENT experiment constrain (at 90% CL with a free average neutron distribution radius)

$$-61 < \langle r^2_{\nu_e} \rangle < 16 \qquad -11 < \langle r^2_{\nu_\mu} \rangle < 22 \qquad (90\%\ \mathrm{CL})$$

$[10^{-32}\,\mathrm{cm}^2]$

- First constraints on transition charge radii:

$$|\langle r^2_{\nu_{e\mu}} \rangle| < 26 \qquad |\langle r^2_{\nu_{e\tau}} \rangle| < 40 \qquad |\langle r^2_{\nu_{\mu\tau}} \rangle| < 30 \qquad (90\%\ \mathrm{CL})$$

- An improvement of about 1 order of magnitude is necessary to be competitive with the current limits of the order of few $\times\, 10^{-32}\,\mathrm{cm}^2$.

- An improvement of about 2 orders of magnitude is necessary to reach the Standard Model values

$$\langle r^2_{\nu_e} \rangle_{\mathrm{SM}} = -8.2 \times 10^{-33}\,\mathrm{cm}^2 \qquad \langle r^2_{\nu_\mu} \rangle_{\mathrm{SM}} = -4.8 \times 10^{-33}\,\mathrm{cm}^2$$

- The new CEνNS experiments may allow to approach these values.

Magnetic and Electric Moments

- Extended Standard Model with right-handed neutrinos and $\Delta L = 0$:

$$\mu^{\text{D}}_{kk} \simeq 3.2 \times 10^{-19} \mu_{\text{B}} \left(\frac{m_k}{\text{eV}} \right) \qquad \varepsilon^{\text{D}}_{kk} = 0$$

$$\left.\begin{matrix} \mu^{\text{D}}_{kj} \\ i\varepsilon^{\text{D}}_{kj} \end{matrix}\right\} \simeq -3.9 \times 10^{-23} \mu_{\text{B}} \left(\frac{m_k \pm m_j}{\text{eV}} \right) \sum_{\ell=e,\mu,\tau} U^*_{\ell k} U_{\ell j} \left(\frac{m_\ell}{m_\tau} \right)^2$$

off-diagonal moments are GIM-suppressed

[Fujikawa, Shrock, PRL 45 (1980) 963; Pal, Wolfenstein, PRD 25 (1982) 766; Shrock, NPB 206 (1982) 359; Dvornikov, Studenikin, PRD 69 (2004) 073001, JETP 99 (2004) 254]

- Extended Standard Model with Majorana neutrinos ($|\Delta L| = 2$):

$$\mu^{\text{M}}_{kj} \simeq -7.8 \times 10^{-23} \mu_{\text{B}} \, i \, (m_k + m_j) \sum_{\ell=e,\mu,\tau} \text{Im} \left[U^*_{\ell k} U_{\ell j} \right] \frac{m_\ell^2}{m_W^2}$$

$$\varepsilon^{\text{M}}_{kj} \simeq 7.8 \times 10^{-23} \mu_{\text{B}} \, i \, (m_k - m_j) \sum_{\ell=e,\mu,\tau} \text{Re} \left[U^*_{\ell k} U_{\ell j} \right] \frac{m_\ell^2}{m_W^2}$$

[Shrock, NPB 206 (1982) 359]

GIM-suppressed, but additional model-dependent contributions of the scalar sector can enhance the Majorana transition dipole moments

[Pal, Wolfenstein, PRD 25 (1982) 766; Barr, Freire, Zee, PRL 65 (1990) 2626; Pal, PRD 44 (1991) 2261]

Method	Experiment	Limit $[\mu_B]$	CL	Year
Reactor $\bar{\nu}_e\, e^-$	Krasnoyarsk	$\mu_{\nu_e} < 2.4 \times 10^{-10}$	90%	1992
	Rovno	$\mu_{\nu_e} < 1.9 \times 10^{-10}$	95%	1993
	MUNU	$\mu_{\nu_e} < 9 \times 10^{-11}$	90%	2005
	TEXONO	$\mu_{\nu_e} < 7.4 \times 10^{-11}$	90%	2006
	GEMMA	$\mu_{\nu_e} < 2.9 \times 10^{-11}$	90%	2012
Accelerator $\nu_e\, e^-$	LAMPF	$\mu_{\nu_e} < 1.1 \times 10^{-9}$	90%	1992
Accelerator $(\nu_\mu, \bar{\nu}_\mu)\, e^-$	BNL-E734	$\mu_{\nu_\mu} < 8.5 \times 10^{-10}$	90%	1990
	LAMPF	$\mu_{\nu_\mu} < 7.4 \times 10^{-10}$	90%	1992
	LSND	$\mu_{\nu_\mu} < 6.8 \times 10^{-10}$	90%	2001
Accelerator $(\nu_\tau, \bar{\nu}_\tau)\, e^-$	DONUT	$\mu_{\nu_\tau} < 3.9 \times 10^{-7}$	90%	2001
Solar $\nu_e\, e^-$	Super-Kamiokande	$\mu_S(E_\nu \gtrsim 5\,\text{MeV}) < 1.1 \times 10^{-10}$	90%	2004
	Borexino	$\mu_S(E_\nu \lesssim 1\,\text{MeV}) < 2.8 \times 10^{-11}$	90%	2017

[see the review CG, Studenikin, RMP 87 (2015) 531, arXiv:1403.6344]

- Gap of about 8 orders of magnitude between the experimental limits and the $\lesssim 10^{-19}\,\mu_B$ prediction of the minimal Standard Model extensions.
- $\mu_\nu \gg 10^{-19}\,\mu_B$ discovery $\Rightarrow$ non-minimal new physics beyond the SM.
- Neutrino spin-flavor precession in a magnetic field

[Lim, Marciano, PRD 37 (1988) 1368; Akhmedov, PLB 213 (1988) 64]

- Neutrino magnetic (and electric) moment contributions to CEνNS $\nu_\ell + \mathcal{N} \to \sum_{\ell'} \nu_{\ell'} + \mathcal{N}$:

$$\frac{d\sigma_{\nu_\ell\text{-}\mathcal{N}}}{dT}(E_\nu, T) = \frac{G_{\text{F}}^2 M}{\pi} \left(1 - \frac{MT}{2E_\nu^2}\right) \left[g_V^n N F_N(|\vec{q}|^2) + g_V^p Z F_Z(|\vec{q}|^2)\right]^2 + \frac{\pi\alpha^2}{m_e^2} \left(\frac{1}{T} - \frac{1}{E_\nu}\right) Z^2 F_Z^2(|\vec{q}|^2) \sum_{\ell' \neq \ell} \frac{|\mu_{\ell\ell'}|^2}{\mu_{\text{B}}^2}$$

- The magnetic moment interaction adds incoherently to the weak interaction because it flips helicity.

- The m_e is due to the definition of the Bohr magneton: $\mu_{\text{B}} = e/2m_e$.

Cross sections averaged over the COHERENT neutrino energy spectra

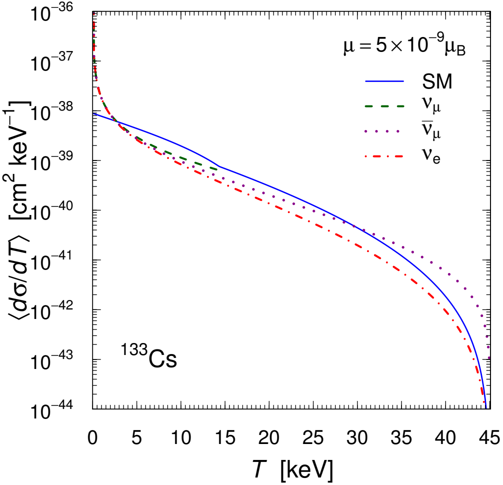

- The COHERENT energy threshold is about 4 keV.
- It is possible to constrain μ_ν only at the level of a few $\times 10^{-9} \mu_B$.
- It is about 2 orders of magnitude larger than the best upper bound on μ_{ν_e}.
- It is only about 1 order of magnitude larger than the best upper bound on μ_{ν_μ}.

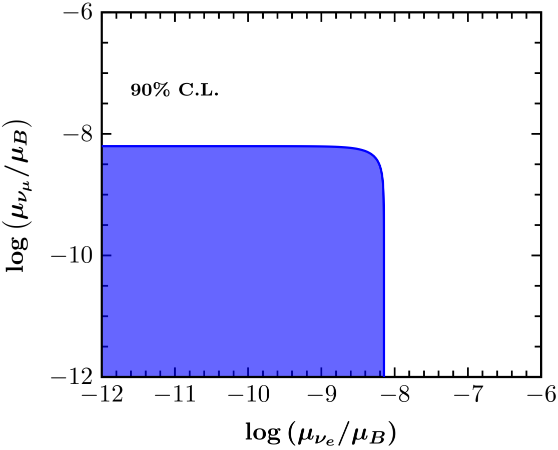

[Papoulias, Kosmas, PRD 97 (2018) 033003, arXiv:1711.09773]

Conclusions

- The observation of CEνNS in the COHERENT experiment opened the way for new powerful measurements of the properties of nuclei and neutrinos.
- We obtained the first determination of R_n with ν-nucleus scattering.
- We constrained the neutrino charge radii and obtained the first constraints on the transition charge radii.
- An improvement of about 1 order of magnitude is necessary to be competitive with the current limits on $\langle r^2_{\nu_e} \rangle$ and $\langle r^2_{\nu_\mu} \rangle$.
- An improvement of about 2 orders of magnitude is necessary to reach the Standard Model values of $\langle r^2_{\nu_e} \rangle$ and $\langle r^2_{\nu_\mu} \rangle$.
- The COHERENT data constrain also the neutrino magnetic moments.
- An improvement of about 2 orders of magnitude is necessary to be competitive with the current limits on μ_{ν_e}.
- An improvement of only 1 order of magnitude is necessary to be competitive with the current limits on μ_{ν_μ}.
- The new CEνNS experiments may allow to approach these goals.